The premolten layer of ice next to a hydrophilic solid surface: correlating adhesion with molecular properties

Jonathan F. D. Liljeblad, István Furó, Eric Tyrode[*]

Department of Chemistry, School of Chemical Science and Engineering, KTH Royal Institute of Technology, SE-100 44 Stockholm, Sweden

[*] Corresponding author: tyrode@kth.se. Telephone: +46 8 7909915

Electronic Supporting Information

*Movie showing the sliding behavior during the adhesion measurement to be find in a separate document file in ESI.

ESI1. Ice adhesion measurement device

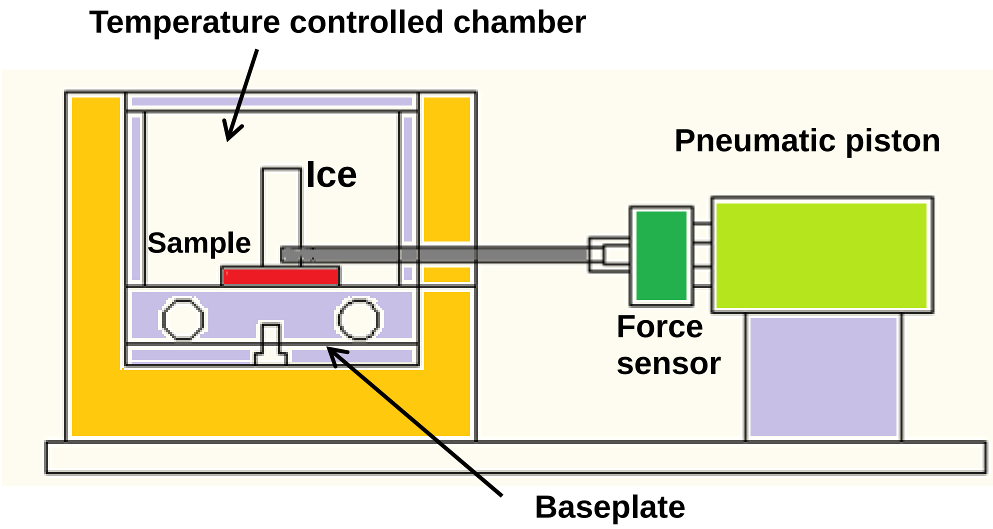

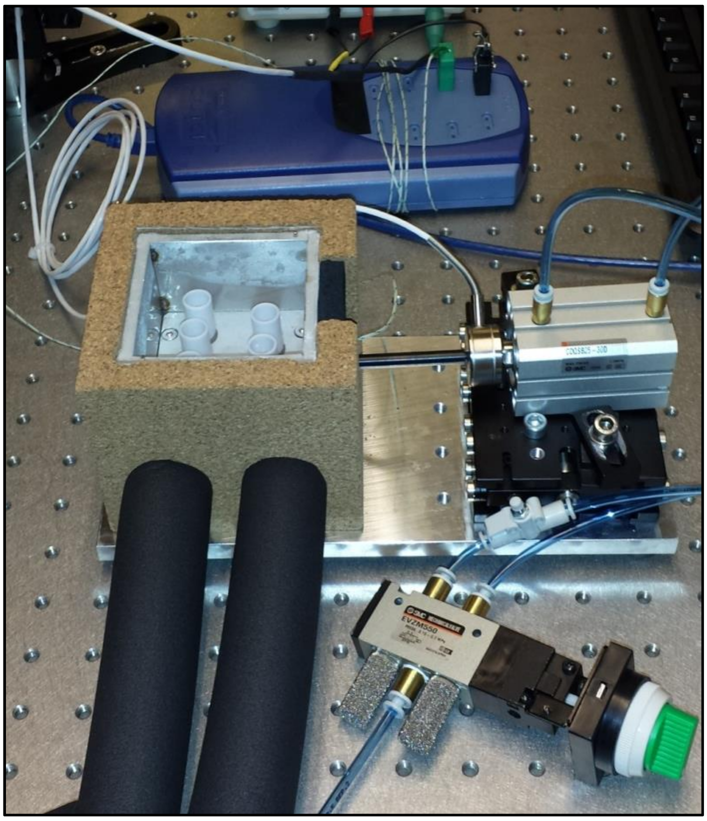

Figure S1. Schematic drawing and photograph showing the ice adhesion measurement device.

ESI2. Ice spectroscopy cell

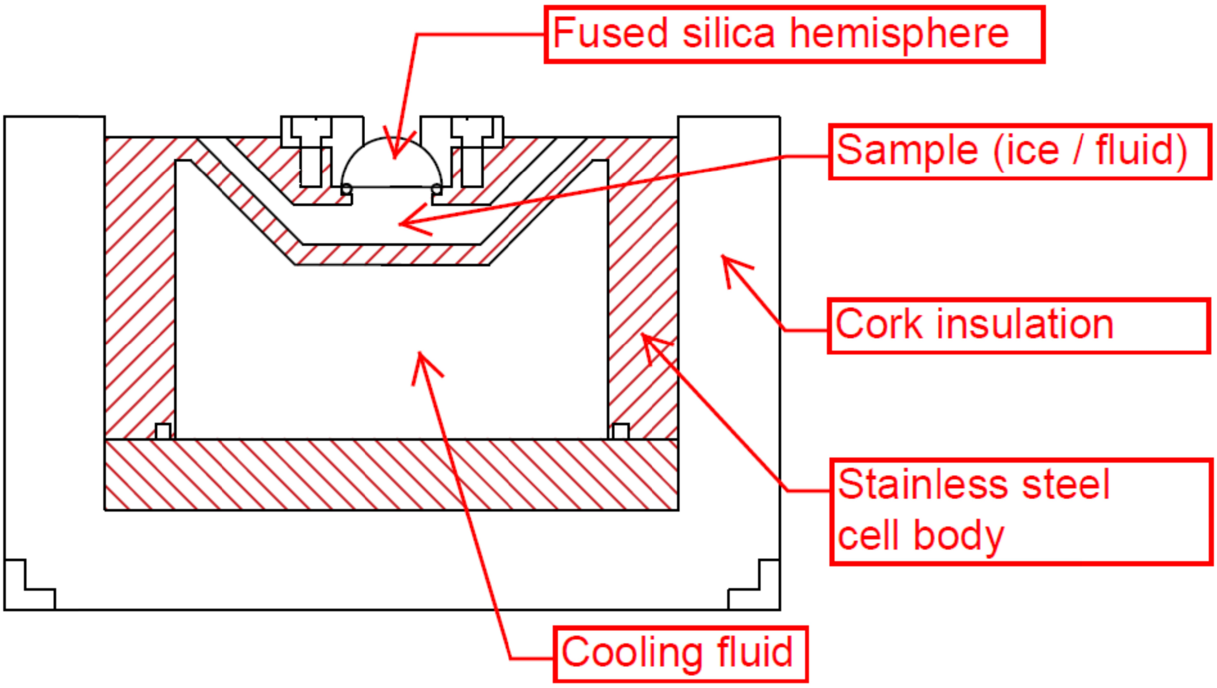

Figure S2. Schematic drawing and photograph showing the ice spectroscopy cell. When in use, the top part, except the slit where the laser beam enters, is covered with additional cork insulation.

ESI3. TIR Raman spectra of bulk H_2O ice

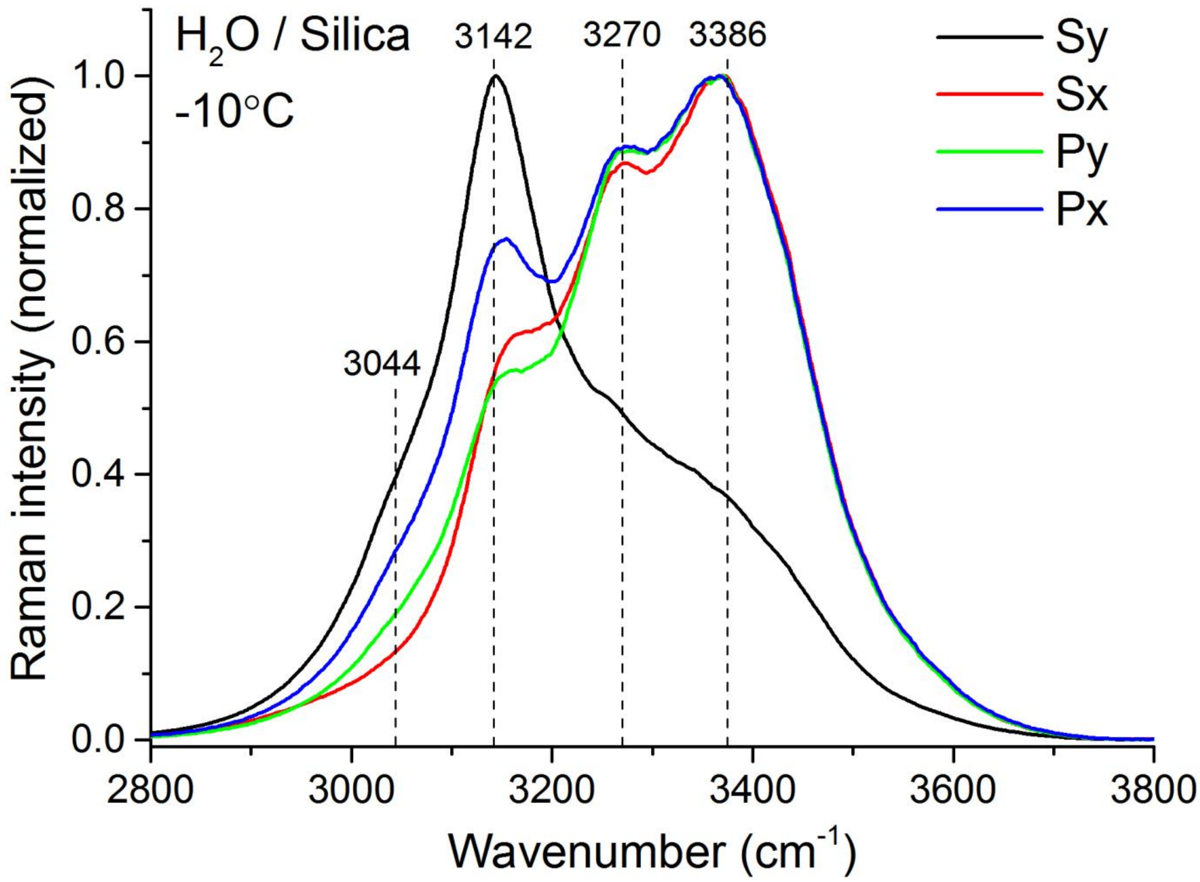

Figure S3. TIR Raman spectra recorded in four different polarization combinations (Sy, Sx, Py, and Px) of bulk H_2O ice at -10°C. The spectra have been normalized so that the intensity of the highest intensity peak equals one. The peak positions are based on a fitting to Lorentzian line shape functions (see **Figure S4**).

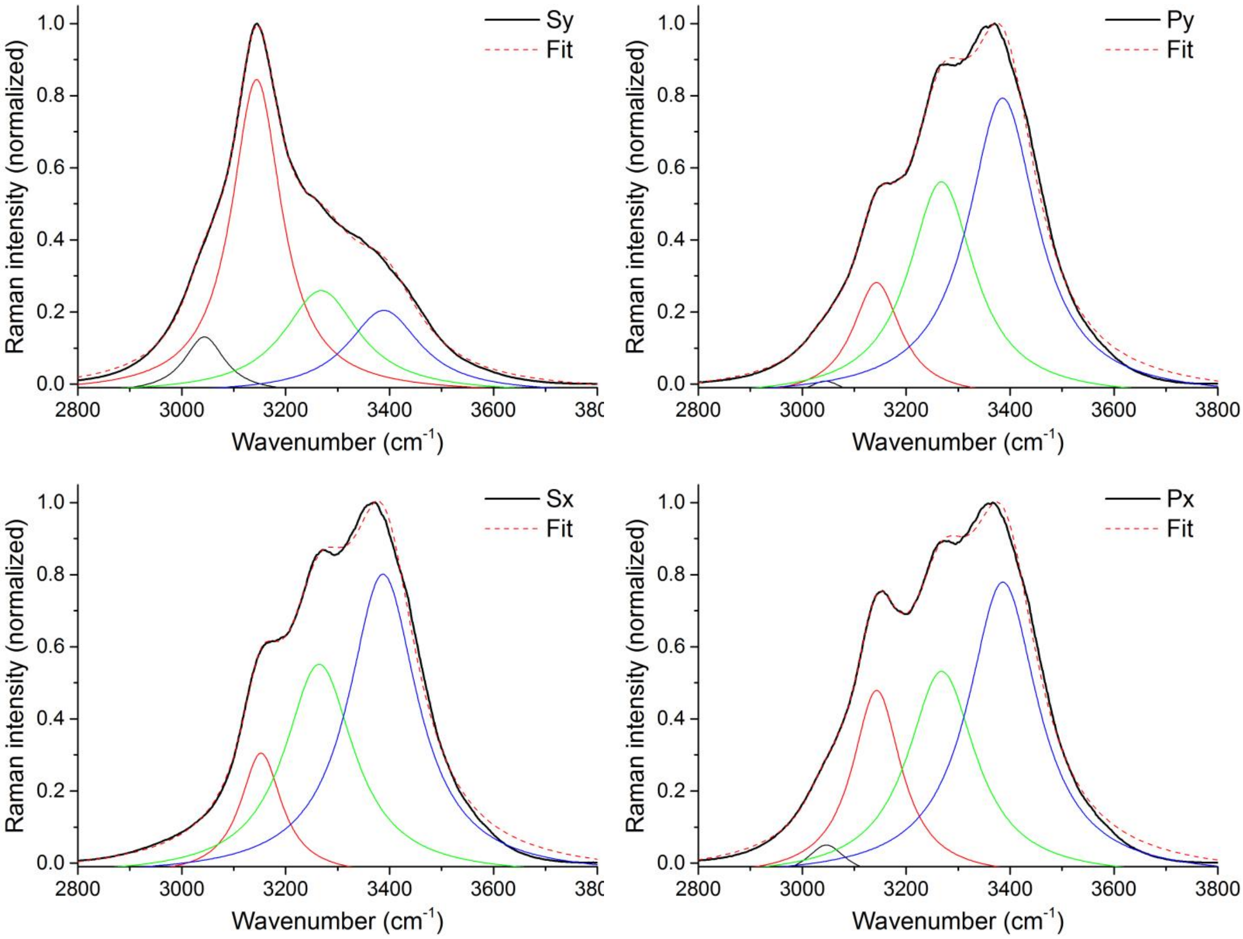

Figure S4. TIR Raman spectra of bulk H_2O ice recorded at -10°C in the Sy, Sx, Py, and Px polarization combinations. The spectra were fitted with four Lorentzian line shape functions (colored lines), and the dashed line show the resulting fit. The Sx spectrum was fitted with only three peaks.

ESI4. TIR Raman spectra of D_2O ice

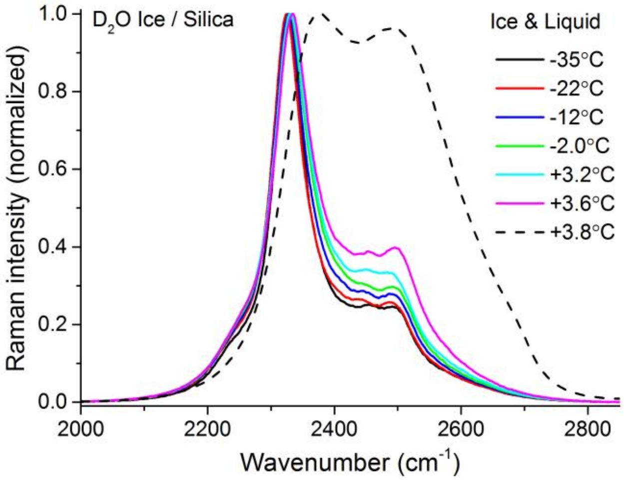

Figure S5. TIR Raman spectra (Sy) of bulk D_2O ice (melting temperature +3.8°C) at various temperatures ranging from -35°C to +3.6°C (solid lines) and liquid D_2O at the melting temperature (dashed line). The ice spectra have been normalized to the peak at approximately 2330 cm^{-1} and the water spectrum to the peak at approximately 2375 cm^{-1}. Note that the spectrum of the liquid was collected under the polarization Sx+Sy (unpolarized collection).

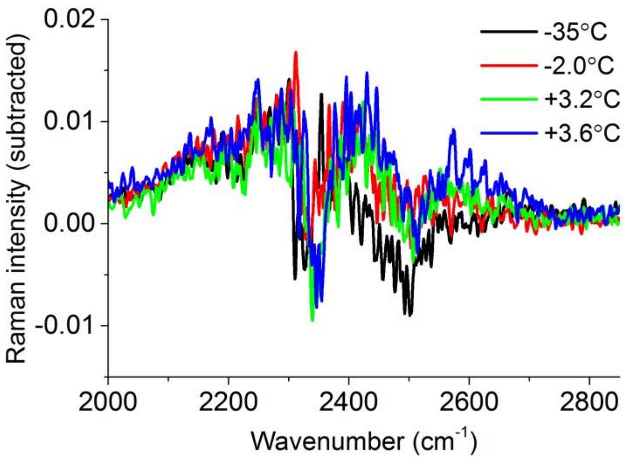

Figure S6. Surface contribution (subtraction of bulk spectrum from 100 nm spectrum for each temperature) of D_2O ice at different temperatures. This figure is shown as an inset in Figure 4 in the main paper.

ESI5. Additional VSFS spectra collected under the SPS polarization combination

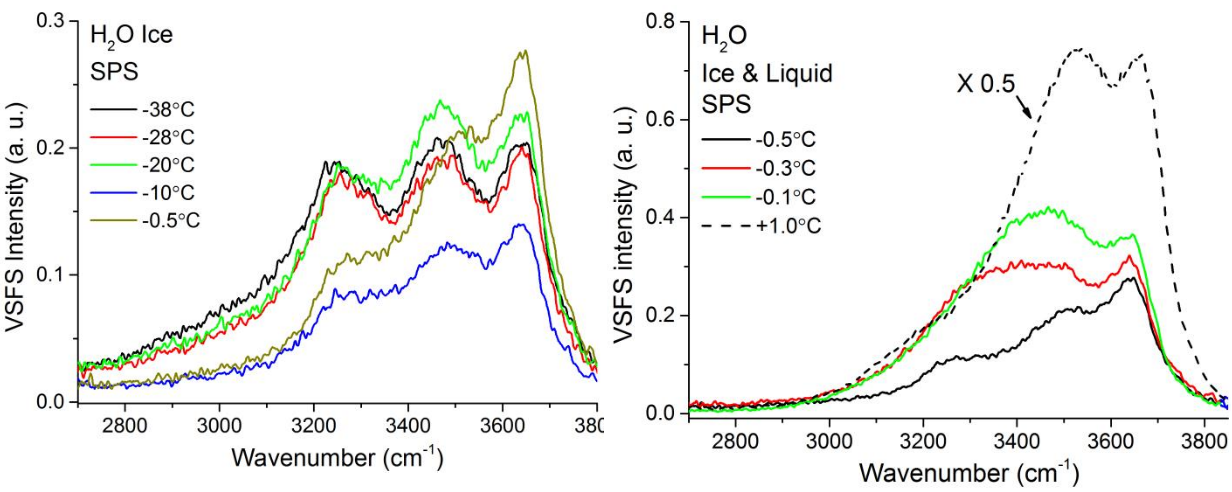

Figure S7. VSF spectra recorded in the SPS polarization combination of H_2O ice at low temperatures (left) and high temperatures (right). The SPS spectrum of liquid water is added as a reference.

ESI6. Fresnel factor correction of VSF spectra

The angle of incidence of the visible and infrared beams chosen in a particular spectrometer, as well as the refractive indexes of the substances forming the interface under investigation, influences the wavenumber dependent intensity of the spectral features.[1] This is rarely accounted for when presenting VSFS data. **Figure S8** shows the curves used for normalizing the spectra to account for those factors, which has been calculating following the same principles as described in a previous publication,[1] invoking all angular and refractive index wavenumber dependents factors. To facilitate the calculations, Voight line-shape functions were fitted to the infrared refractive index data of liquid[2] H_2O and H_2O ice[3], while a Sellmeier equation was used for the silica.[4] While the SSP and SPS polarization combinations only contain contributions from one susceptibility tensor element each (assuming C_{∞}-symmetry of the interface), the PPP is an admixture of four tensor elements. In the curves for the spectral normalization only the zzz-element is included since it is expected to the substantially larger than the other elements.

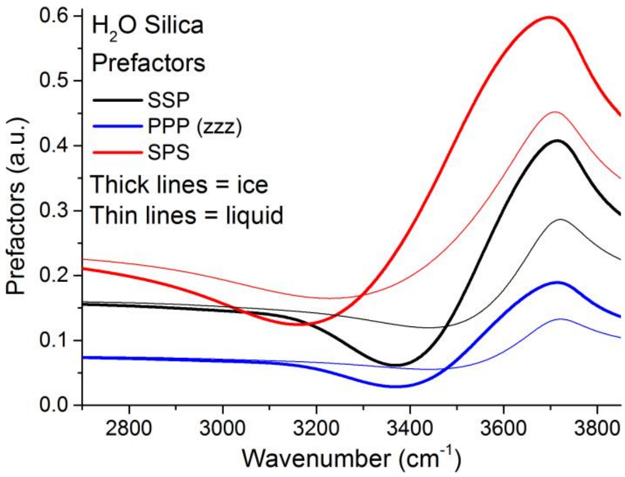

Figure S8. Curves used to normalize the recorded VSF spectra to account for Fresnel factors, as well as refractive index and angle of incidence wavenumber dependent intensity variations. Note, that because the purpose of the normalization was only to correct the shape of each individual spectrum, each curve was divided with its highest value to set it to one, and the intensity difference between the different polarization combinations was thus not taken into account.

[1] Liljeblad, J. F. D.; Tyrode, E. *Journal of Physical Chemistry C* **2012**, *116*, 22893.

[2] Max, J. J.; Chapados, C. *J Chem Phys* **2009**, *131*, 184505.

[3] Warren, S. G.; Brandt, R. E. *J Geophys Res-Atmos* **2008**, *113*.

[4] Malitson, I. H. *J. Opt. Soc. Am.* **1965**, *55*, 1205.

ESI7. Fresnel factors corrected VSF spectra

The figures in this section corresponds to Figures 6, 7, and 8, in the main paper, which here have been corrected to account for the refractive index and experimental geometry dependent factors as described in the previous section. The number(s) within parenthesis after each figure number denotes the corresponding figure number in the main paper.

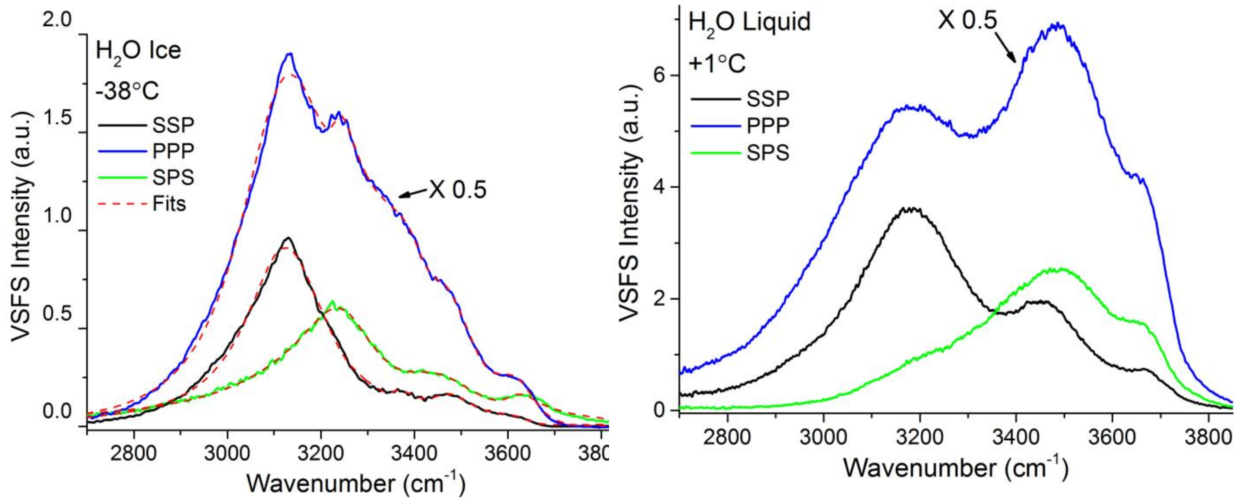

Figure S9; (6a, 6b). Fresnel factors corrected VSF spectra recorded in the SSP, PPP, and SPS polarization combinations of H_2O ice at -38°C (left) and H_2O liquid at +1°C (right). Note that the intensity in the PPP spectra has been divided by 2 for ease of comparison. Red dashed lines in Figure S9 (left) are fits to the spectra.

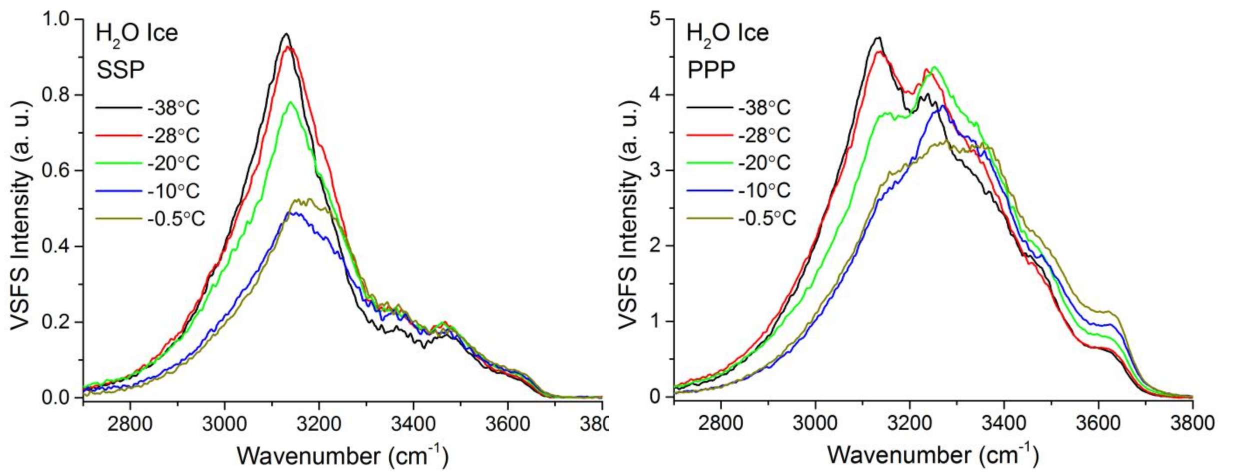

Figure S10; (7a, 7b). Fresnel factors corrected VSF spectra recorded in the SSP (left), and PPP (right) polarization combinations of H_2O ice in contact with fused silica at various temperatures ranging from -38°C and -0.5°C.

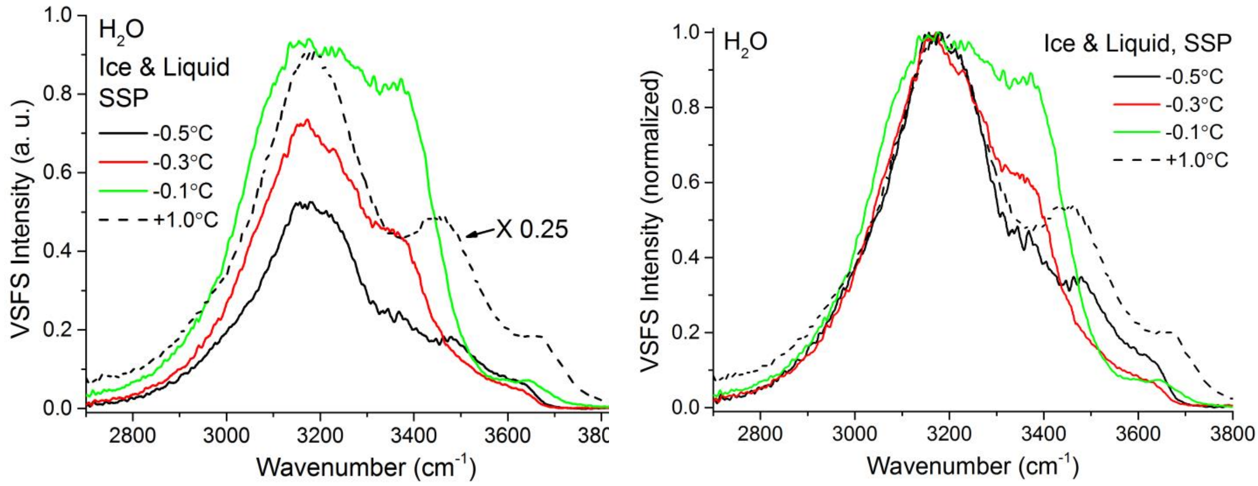

Figure S11; (left 8). Left: Fresnel factors corrected VSF spectra recorded in the SSP polarization combinations of H_2O ice in contact with fused silica at various temperatures ranging from -0.5°C and -0.1°C. The corresponding Fresnel factor corrected spectrum for liquid water is also added for reference. **Right:** Same SSP spectra but normalized to the highest peak in the spectrum and where it is easier to appreciate changes in the relative spectral features upon increase of temperature.

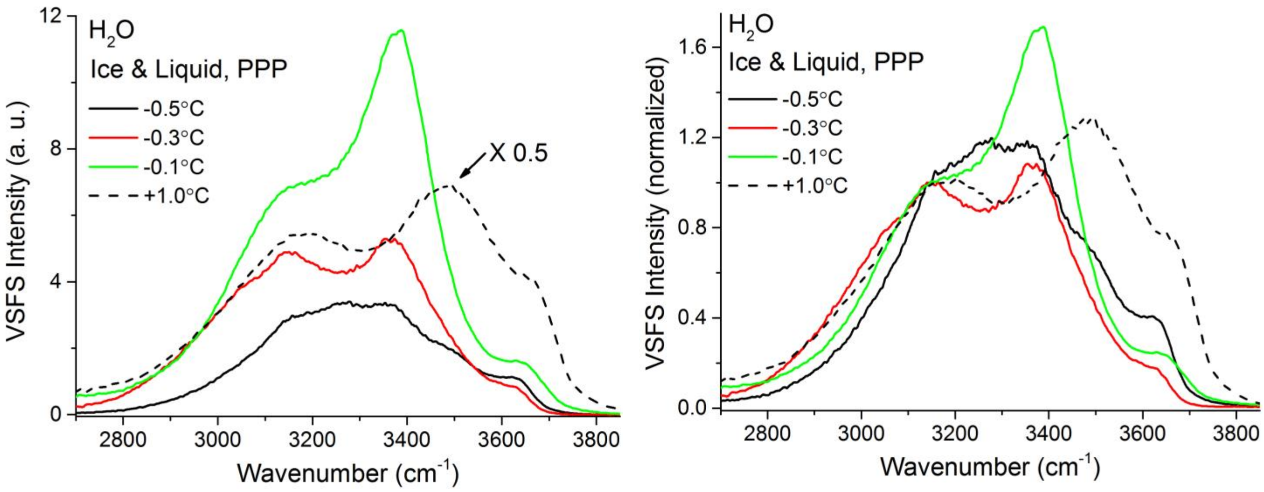

Figure S12; (right 8). Left: Fresnel factors corrected VSF spectra recorded in the PPP polarization combinations of H_2O ice in contact with fused silica at various temperatures ranging from -0.5°C and -0.1°C. The corresponding Fresnel factor corrected spectrum for liquid water is also added for reference. **Right:** same PPP spectra but normalized to the ~3140 cm^{-1} peak to better appreciate changes in the relative spectral features upon increase of temperature.

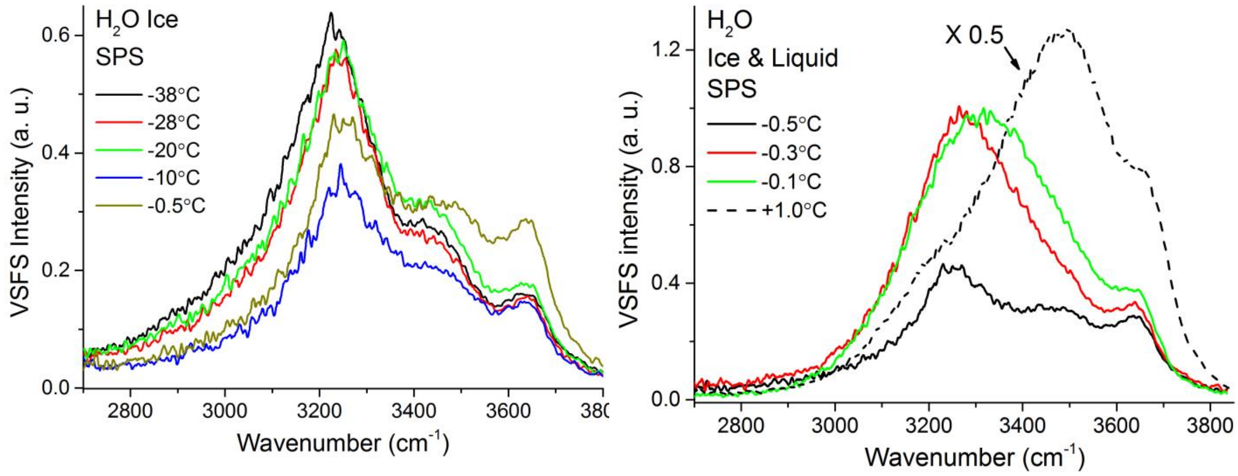

Figure S13; (uncorrected data in Figure S7). Fresnel factors corrected VSF spectra recorded in the SPS polarization combinations of H_2O ice in contact with fused silica at various temperatures ranging from -38°C and -0.5°C (left) and between -0.5°C and -0.1°C (right). The corresponding Fresnel factor corrected spectrum for liquid water is also added for reference (see dashed line on the spectra to the right).

ESI8. Profilometry data

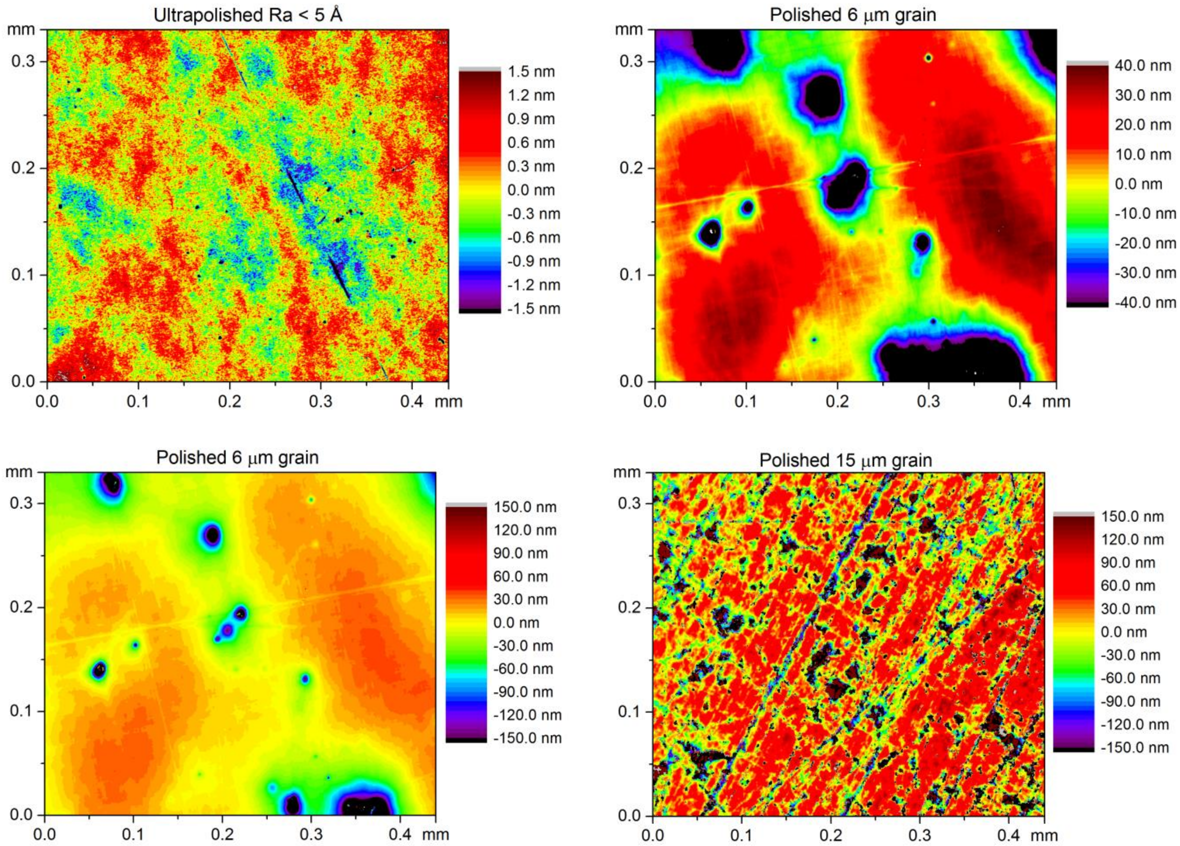

Figure S14. Profilometer-images of silica discs used for adhesion measurements. The top left image shows an as received ultra-polished silica disc (Ra < 4 Å) after repeated ice adhesion measurements, the bottom right image shows a disc polished with 15 εm grain sandpaper, and the remaining images (using different color scales) show a disc polished with 6 εm grain size diamond paste after 15 εm grain sandpaper.

Table 1. Roughness parameters extracted from the profilometer-images in Figure **S14**.

	0.33 x 0.44 mm	
	Ra [nm]	**Rq [nm]**
As received	0.40	0.55
6 εm	22	38
15 εm	80	190

ESI9. AFM

Silica disc as received (Ra < 4 Å) after adhesion measurements.

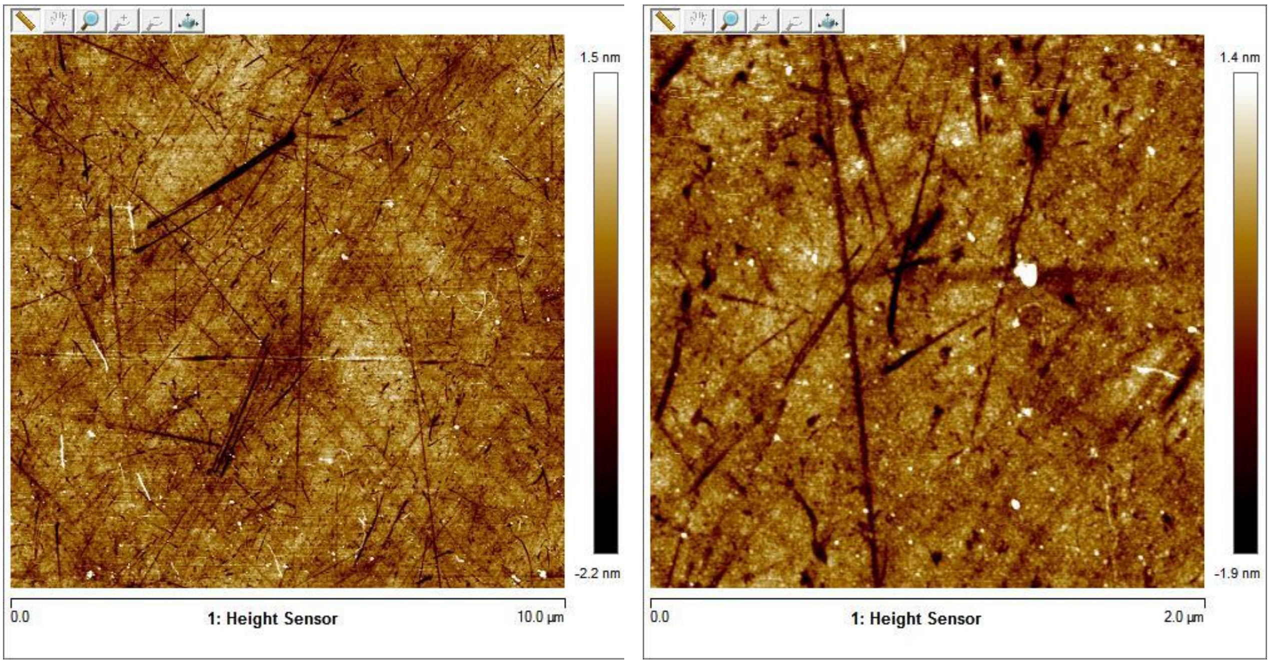

Silica disc polished with 6 εm diamond paste after 15 εm grain sandpaper.

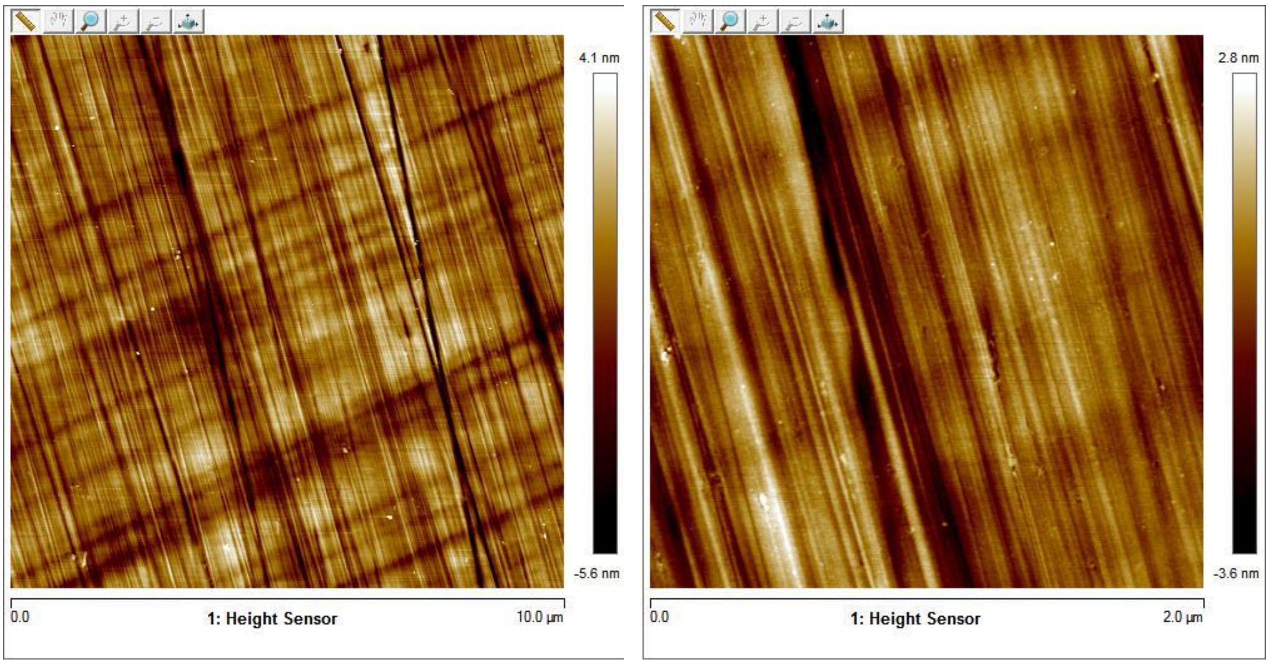

Silica disc polished with 15 εm grain sandpaper

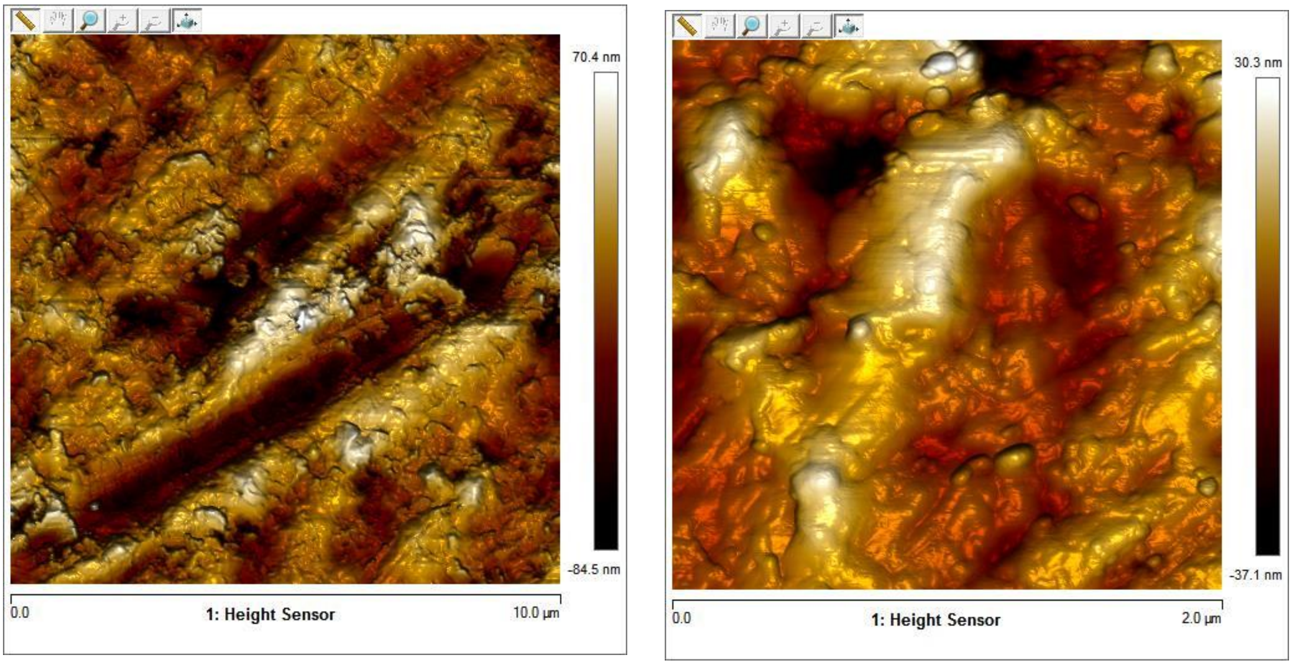

Figure S15. AFM-images of silica discs used for adhesion measurements. The left column shows 10 x 10 εm images and the right column 2 x 2 εm images. The top row shows as received ultra-polished silica discs (Ra < 4 Å) after repeated ice adhesion measurements, the bottom row shows discs polished with 15 εm grain sandpaper, and the middle row shows discs polished with 6 εm grain size diamond paste after 15 εm grain sandpaper.

Table 2. Roughness parameters extracted from the AFM-images in Figure **S15**.

	10 x 10 εm		**2 x 2 εm**	
	Ra [nm]	**Rq [nm]**	**Ra [nm]**	**Rq [nm]**
As received	0.33	0.49	0.29	0.45
6 εm	0.95	1.3	0.66	0.87
15 εm	16	21	6.3	8.4

ESI10. NMR

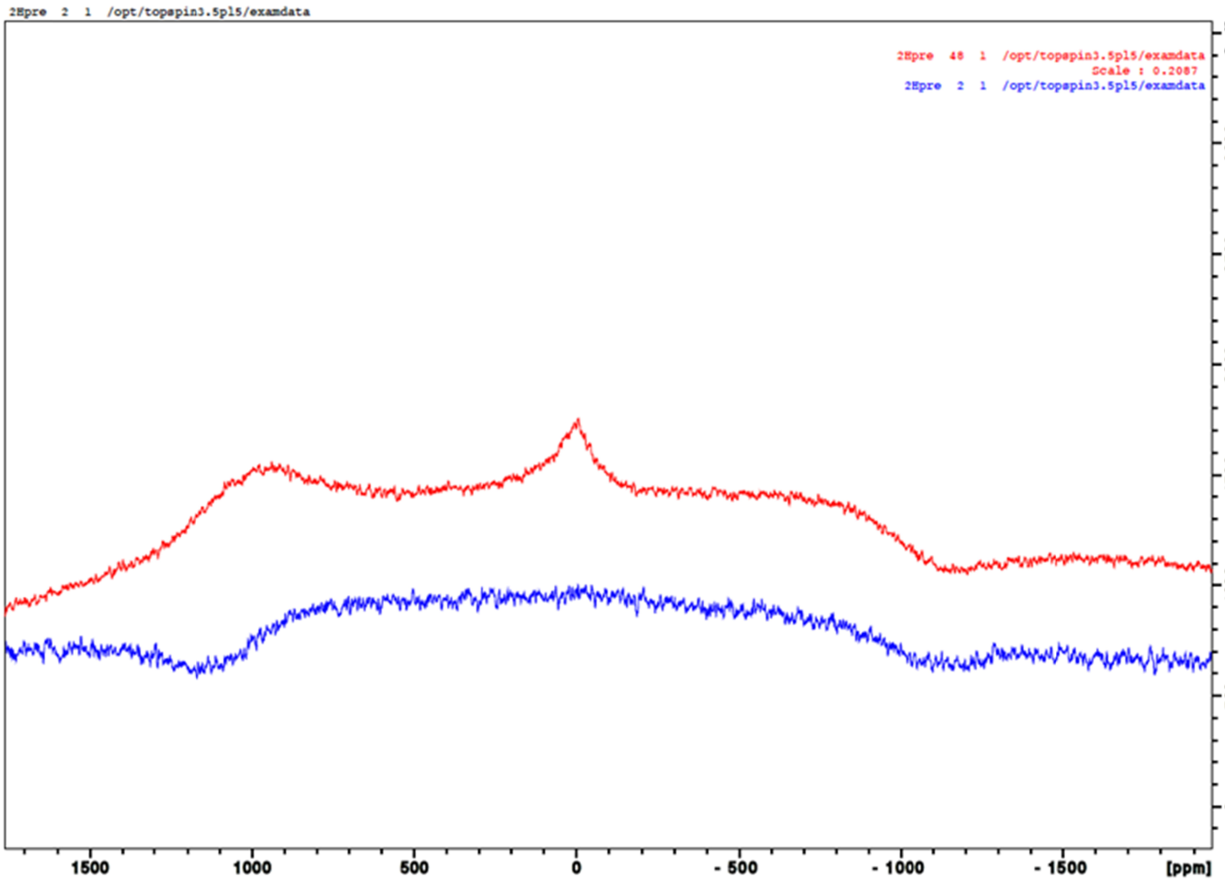

Figure S18. The ^{2}H NMR spectrum of bulk D_2O ice (blue) and D_2O imbibed in the explored controlled pore glass, both recorded at -10^{o}C in a single-pulse experiment with *ca* 11^o excitation pulse of 1 εs pulse length. The intensity of the central peak (that is exclusive to the controlled pore glass sample at the different explored temperatures below the pore freezing point) is associated with the extent of the PML. The 90^o edges of the broad ^{2}H powder pattern that arises from solid ice are manifested as humps on the two sides.

ESI11. SF fitting parameters

The parameters obtained from fitting the VSF spectra of ice to Equation (1) in the main paper are collected in the tables below (**Table S3 -**

Table S5). Before fitting, the spectra were corrected by division with the normalization curves (Fresnel factor corrections) in **Figure S8**. It must be stressed that given the large number of parameters (for instance 3 x 6 + 1 for a spectrum fitted with six peaks) multiple local minima exist. Based on our practical experience, the presented parameters are not deemed to be a unique fit, nor necessarily representing a global minimum (i.e. the best possible fit) in the parameter space. The final result obtained from a particular fitting sequence depends on factors such as the starting guess, and the settings used in the Levenberg-Marquardt algorithm employed. In addition, parameters have sometimes been constrained to prevent unphysical, or otherways unreasonable, fitting results. Those constrained parameters are highlighted with italics in the tables.

As can be inferred from visual inspection of the spectra the peak widths (Γ) varies as the temperature of the ice changes. To enable comparisons of the intensities (A_n) of individual peaks presented in Figure 9 in the main paper, they were corrected by dividing by the corresponding peak widths (Γ_n) as can be justified from Equation (79) in a review by Lambert et. al.[5]

[5] Lambert, A. G.; Davies, P. B.; Neivandt, D. J. *Applied Spectroscopy Reviews* **2005**, *40*, 103.

Table S3. Fitting parameters for the spectra in the SSP polarization combination.

Temp [°C]	A_1	ω_1	Γ_1	A_2	ω_2	Γ_2	A_3	ω_3	Γ_3
-38	10	3122	105	-0.093	*3240*	*35*	0.16	3361	25
-28	11	3136	114	-0.007	*3240*	*35*	0.19	3359	27
-20	11	3140	123	0.017	*3240*	*35*	0.20	3360	30
-10	10	3139	138	0.079	*3240*	*35*	0.13	3359	27
-5.0	8.6	3155	126	0.28	*3240*	*35*	0.07	3365	24
-2.0	8.6	3162	127	0.21	*3240*	*35*	0.16	3375	33
-1.0	8.7	3153	130	0.15	*3240*	*35*	0.08	3362	21
-0.5	9.2	3159	128	0.20	*3240*	*35*	0.17	3362	30
-0.25	12	3138	138	0.068	*3240*	*35*	-0.14	3405	27
-0.05	10	3104	124	3.1	3210	106	-4.7	3424	76

Temp [°C]	A_4	ω_4	Γ_4	A_5	ω_5	Γ_5	A_6	ω_6	Γ_6
-38	0.74	3455	52	-1.4	*3510*	*90*	-0.53	3635	46
-20	0.77	3457	56	-1.6	*3510*	*90*	-0.77	3641	53
-28	0.76	3455	52	-1.5	*3510*	*90*	-0.56	3640	46
-10	0.38	3459	47	-1.5	*3510*	*90*	-1.0	3639	60
-5.0	0.79	3471	59	-1.6	*3510*	*90*	-0.87	3644	52
-2.0	0.39	3466	41	-1.4	*3510*	*90*	-0.90	3646	54
-1.0	1.0	3478	65	-2.1	*3510*	*90*	-0.86	3644	51
-0.5	0.89	3474	61	-2.0	*3510*	*90*	-0.86	3645	53
-0.25	-1.1	3430	63	-1.5	*3510*	*90*	-1.0	3630	68
-0.05	-0.09	3470	23	-1.6	*3510*	*90*	-1.4	3641	70

Temp [°C]	A_{NR}	A_1/Γ_1	A_2/Γ_2	A_3/Γ_3	A_4/Γ_4	A_5/Γ_5	A_6/Γ_6
-38	-0.00021	0.10	-0.0027	0.0065	0.014	-0.015	-0.012
-28	0.00059	0.10	-0.00021	0.0070	0.015	-0.017	-0.012
-20	0.0005	0.086	0.00049	0.0067	0.014	-0.017	-0.015
-10	-0.0027	0.069	0.0023	0.0050	0.0080	-0.017	-0.017
-5.0	-0.0019	0.068	0.0081	0.0029	0.013	-0.018	-0.017
-2.0	-0.0023	0.068	0.0061	0.0047	0.009	-0.015	-0.017
-1.0	-0.0028	0.067	0.0042	0.0040	0.015	-0.023	-0.017
-0.5	-0.0022	0.072	0.0058	0.0058	0.015	-0.022	-0.016
-0.25	-0.0054	0.084	0.0020	-0.0052	-0.018	-0.017	-0.015
-0.05	0.00052	0.082	0.02935	-0.062	-0.0042	-0.017	-0.020

Table S4. Fitting parameters for the spectra in the PPP polarization combination.

Temp [°C]	A_1	ω_1	Γ_1	A_2	ω_2	Γ_2	A_3	ω_3	Γ_3
-38	28	3110	133	0.60	3236	27	-2.6	3409	64
-28	32	3116	155	0.47	3237	24	-3.9	3405	79
-20	33	3130	178	0.65	3240	30	-5.3	3407	84
-10	28	3136	177	1.22	3240	43	-6.6	3414	89
-5.0	27	3114	192	0.67	3236	42	-6.6	3414	84
-2.0	28	3134	188	0.50	3239	38	-7.3	3414	88
-1.0	28	3139	185	0.29	3237	31	-6.4	3418	91
-0.5	29	3129	188	0.15	3245	*35*	-6.0	3419	83
-0.25	43	3129	188	-0.57	3245	*35*	-20.5	3419	83
-0.05	43	3096	172	0.01	3245	*35*	-17.9	3405	70

Temp [°C]	A_4	ω_4	Γ_4	A_5	ω_5	Γ_5	A_6	ω_6	Γ_6
-38	-3.3	3494	58	-2.0	3552	63	-3.4	3635	56
-28	-3.6	3499	71	-2.0	3553	66	-3.4	3641	57
-20	-3.7	3501	64	-1.9	3555	*65*	-4.5	3639	61
-10	-2.3	3507	54	-2.7	3559	*65*	-4.4	3640	56
-5.0	-3.3	3503	*60*	-2.7	3560	*65*	-3.9	3637	54
-2.0	-3.3	3505	60	-2.7	3565	*65*	-4.0	3638	55
-1.0	-2.4	3507	*55*	-2.9	3562	*65*	-4.3	3639	55
-0.5	-2.6	3507	*55*	-2.9	3562	*65*	-4.7	3640	55
-0.25	-4.1	3507	*55*	2.7	3562	*65*	-2.0	3630	41
-0.05	-6.1	3463	58	-5.2	3538	68	-2.7	3625	43

Temp [°C]	A_{NR}	A_1/Γ_1	A_2/Γ_2	A_3/Γ_3	A_4/Γ_4	A_5/Γ_5	A_6/Γ_6
-38	-0.013	0.21	0.022	-0.041	-0.057	-0.032	-0.061
-28	-0.013	0.21	0.019	-0.050	-0.051	-0.026	-0.060
-20	-0.015	0.19	0.022	-0.063	-0.057	-0.029	-0.074
-10	-0.020	0.16	0.028	-0.074	-0.042	-0.042	-0.078
-5.0	-0.024	0.14	0.016	-0.079	-0.056	-0.042	-0.072
-2.0	-0.023	0.15	0.013	-0.084	-0.055	-0.042	-0.073
-1.0	-0.021	0.15	0.0095	-0.070	-0.043	-0.045	-0.079
-0.5	-0.025	0.16	0.0044	-0.073	-0.047	-0.045	-0.085
-0.25	0.011	0.23	-0.016	-0.248	-0.074	0.042	-0.050
-0.05	0.0089	0.25	0.00029	-0.257	-0.105	-0.076	-0.062

Table S5. Fitting parameters for the spectra in the SPS polarization combination.

Temp [°C]	A_1	ω_1	Γ_1	A_2	ω_2	Γ_2	A_3	ω_3	Γ_3
-38	1.4	3140	150	6.4	3250	106	3.7	3442	118
-28	0.012	3140	150	6.2	3261	105	4.2	3451	125
-20	0.096	3140	150	5.9	3264	106	5.0	3447	129
-10	-1.9	3140	150	3.9	3278	105	5.6	3469	152
-5.0	-2.2	3140	150	3.3	3288	105	6.9	3491	162
-2.0	-2.4	3140	150	3.8	3289	111	6.4	3495	146
-1.0	-2.5	3140	150	3.5	3294	101	6.8	3491	146
-0.5	-2.5	3140	150	3.8	3289	102	7.2	3489	151
-0.25	-7.3	3140	150	7.4	3327	132	5.6	3478	132
-0.05	-9.0	3140	150	4.1	3390	108	5.6	3509	117

Temp [°C]	A_4	ω_4	Γ_4	A_{NR}	A_1 / Γ_1	A_2 / Γ_2	A_3 / Γ_3	A_4 / Γ_4
-38	0.58	3615	42	0.0059	0.0092	0.060	0.031	0.014
-28	0.58	3619	41	0.0072	0.0001	0.059	0.033	0.014
-20	0.64	3617	43	0.0080	0.0006	0.055	0.039	0.015
-10	0.76	3628	47	0.0096	0.013	0.037	0.037	0.016
-5.0	1.2	3635	50	0.012	0.015	0.031	0.043	0.024
-2.0	1.1	3634	50	0.011	0.016	0.034	0.043	0.022
-1.0	1.5	3634	53	0.013	0.017	0.035	0.047	0.027
-0.5	1.2	3633	51	0.011	0.017	0.038	0.047	0.024
-0.25	2.7	3643	78	0.022	0.048	0.056	0.042	0.035
-0.05	2.8	3648	70	0.021	0.060	0.038	0.048	0.040

(1) Liljeblad, J. F. D.; Tyrode, E. *Journal of Physical Chemistry C* **2012**, *116*, 22893.

(2) Max, J. J.; Chapados, C. *J Chem Phys* **2009**, *131*, 184505.

(3) Warren, S. G.; Brandt, R. E. *J Geophys Res-Atmos* **2008**, *113*.

(4) Malitson, I. H. *J. Opt. Soc. Am.* **1965**, *55*, 1205.

(5) Lambert, A. G.; Davies, P. B.; Neivandt, D. J. *Applied Spectroscopy Reviews* **2005**, *40*, 103.